NeuroImage 257 (2022) 119322

Contents lists available at ScienceDirect

NeuroImage

journal homepage: www.elsevier.com/locate/neuroimage

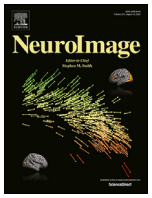

Disentangling performance-monitoring signals encoded in feedback-related EEG dynamics

Franziska Kirsch[a,1,*], Hans Kirschner[a,1], Adrian G. Fischer[a,b,c], Tilmann A. Klein[a,b,d,2], Markus Ullsperger[a,b,2]

[a] Institute of Psychology, Otto-von-Guericke University, Universitätsplatz 2, Magdeburg 39106, Germany
[b] Center for Behavioral Brain Sciences, Universitätsplatz 2, Magdeburg 39106, Germany
[c] Department of Education and Psychology, Freie Universität Berlin, Habelschwerdter Allee 45, Berlin 14195, Germany
[d] Department of Neurology, Max Planck Institute for Human Cognitive and Brain Sciences, Stephanstrasse 1A, Leipzig 04103, Germany

ARTICLE INFO

Keywords:
EEG
FRN
P3
Reward prediction error (RPE)
Feedback processing
Performance monitoring

ABSTRACT

The feedback-related negativity (FRN) is a well-established electrophysiological correlate of feedback-processing. However, there is still an ongoing debate whether the FRN is driven by negative or positive reward prediction errors (RPE), valence of feedback, or mere surprise. Our study disentangles independent contributions of valence, surprise, and RPE on the feedback-related neuronal signal including the FRN and P3 components using the statistical power of a sample of $N = 992$ healthy individuals. The participants performed a modified time-estimation task, while EEG from 64 scalp electrodes was recorded. Our results show that valence coding is present during the FRN with larger amplitudes for negative feedback. The FRN is further modulated by surprise in a valence-dependent way being more positive-going for surprising positive outcomes. The P3 was strongly driven by both global and local surprise, with larger amplitudes for unexpected feedback and local deviants. Behavioral adaptations after feedback and FRN just show small associations. Results support the theory of the FRN as a representation of a signed RPE. Additionally, our data indicates that surprising positive feedback enhances the EEG response in the time window of the P3. These results corroborate previous findings linking the P3 to the evaluation of PEs in decision making and learning tasks.

1. Introduction

In general, feedback is important for learning and adaptive, goal-directed behavior. When feedback informs about an action outcome, a feedback-locked sequence of EEG-components consisting of a frontocentrally distributed feedback-related negativity (FRN; Miltner et al., 1997), the frontocentral P3a, and a parietal P3b can be observed (Ullsperger et al., 2014b). The reinforcement learning (RL) theory of Holroyd and Coles (2002) states that the amplitude of the FRN correlates with the reward prediction error (RPE). Indeed, it is proposed by several researchers that the FRN encodes an RPE (Chase et al., 2011; Cohen and Ranganath, 2007; Holroyd and Coles, 2002; Holroyd and Krigolson, 2007; Nieuwenhuis et al., 2004; Sambrook and Goslin, 2015; Ullsperger et al., 2014a), having a stronger deflection when outcome expectation is violated (Chase et al., 2011; Holroyd and Krigolson, 2007; Walsh and Anderson, 2012). More negative RPEs are suggested to be associated with a stronger posterior mesial frontal cortex (pMFC) response (Jocham et al., 2009) and a larger FRN.

According to the RL-theory, unexpected negative outcomes should elicit larger FRNs than expected negative outcomes (San Martín, 2012). Numerous studies have indicated that the FRN amplitude scales with a "signed" RPE: In the case of a worse-than-expected outcome (negative RPE), a strong FRN is elicited, whereas a smaller and weaker FRN is observed after better-than-expected outcomes (positive RPE; Fischer and Ullsperger, 2013; Hajcak et al., 2007; Holroyd and Coles, 2002; Walsh and Anderson, 2012). Expectations are generated by experience and incorporate global values (frequent/infrequent) but can dynamically adjust to recent events, such as local surprise generated by trial micro-structures (Holroyd and Coles, 2002).

Beyond the RL-account, there are alternative approaches suggesting the FRN corresponds to an unsigned RPE signal which is sensitive to unlikely and therefore salient events indicating surprise (independent of the direction of the expectedness violation, Alexander and Brown, 2011;

* Corresponding author.
E-mail addresses: franziska.kirsch@ovgu.de (F. Kirsch), hans.kirschner@ovgu.de (H. Kirschner), adrian.fischer@fu-berlin.de (A.G. Fischer), tilmann.klein@ovgu.de (T.A. Klein), markus.ullsperger@ovgu.de (M. Ullsperger).
[1] These authors contributed equally to this work.
[2] TK and MU should be considered joint senior author.

https://doi.org/10.1016/j.neuroimage.2022.119322.
Received 14 December 2021; Received in revised form 3 May 2022; Accepted 12 May 2022
Available online 14 May 2022.

Donkers and van Boxtel, 2005; Ferdinand et al., 2012; Hauser et al., 2014; Talmi et al., 2013; Walentowska et al., 2019; Yeung et al., 2005). In contrast, some studies show a dependence of the FRN amplitude on valence and postulate that the magnitude of probability is represented later in more parietal components like the P3b (Kamarajan et al., 2009; Sato et al., 2005; Toyomaki and Murohashi, 2005; Yeung and Sanfey, 2004). Since the P3 complex is increased upon low probability events (Johnson, 1986), FRN and P3 correlate with the common factor surprise and therefore, it is possible that the FRN could be overlapped by the P3 (Walsh and Anderson, 2012). Recently, it has been proposed that the FRN effect of being larger for negative as compared to positive feedback is actually driven by a positive deflection following positive outcomes (RewP; Baker and Holroyd, 2011; Foti and Weinberg, 2018; Holroyd et al., 2008; Krigolson, 2018; Proudfit, 2015). Unexpected outcomes are supposed to elicit the ERP component N200, while trials with unexpected rewards elicit a feedback-related positivity (RewP) and, in consequence, the RewP overshadows the effect of the N200. However, given that the positive (RewP) and negative (FRN) deflections overlap in time, it remains unclear which of them captures systematic changes in reward processing best (Gheza et al., 2018). Some authors, in fact, seem to suggest that FRN and RewP represent the same EEG phenomenon, just with opposite sign (Krigolson, 2018; Proudfit, 2015). In this context, we would like to emphasize that the interpretation of results depends on the definition and quantification of the FRN. While some authors quantify the FRN as the loss-minus-win difference wave or the N2-like component following feedback, others suggest a difference between feedback condition-specific components to loss and gain (Cavanagh et al., 2019). In the present study, we are interested in factors that independently influence feedback-related EEG dynamics in the latency range of the FRN (and P300). Therefore, we applied a single-trial regression approach instead of using an ERP quantification method to avoid interpretation issues arising from different approaches. We merely refer to the FRN and P3a/b to guide the reader in terms of latency and topography during which variables of interest modulate the stereotypical ERP sequence after visual feedback (Ullsperger et al., 2014b).

Concerning learning from feedback, larger behavioral adjustments were found after participants received negative compared to positive feedback, which was also reflected in the amplitude of the FRN (Holroyd and Krigolson, 2007). In the same study, the interaction of expectedness and valence of feedback was associated with the extent of behavioral adaptation.

Whereas the FRN is suggested to reflect an early evaluation process involving the calculation of a prediction error, the P3 has been proposed to translate this information into attentional and working memory processes, and to initiate behavioral adaptation (Donchin and Coles, 1998; Polich, 2007; Verleger, 1997; Verleger et al., 1994). The P3 complex consists of two positive ERP deflections, P3a and P3b, which are elicited by potentially action-related stimuli (Ullsperger et al., 2014b). The early frontocentral P3a seems to reflect fast orienting and stimulus-driven attention mechanisms (Kirschner et al., 2021; Ullsperger et al., 2014b), whereas the more sustained parietal P3b has been proposed to be associated with surprise (Donchin and Coles, 1998; Mars et al., 2008) and action value updating (Ullsperger, 2017; Ullsperger et al., 2014b). It is typically found that unexpectedness or negative valence of the feedback give rise to a larger P3b than expected or positive feedback (de Bruijn et al., 2004; Fischer and Ullsperger, 2013; Walentowska et al., 2016). Nevertheless, some sources report no valence effects (Yeung and Sanfey, 2004) or even reverse findings concerning valence (Hajcak et al., 2007; Severo et al., 2018).

Since there is inconsistent evidence about the influence of valence and expectedness (San Martín, 2012) and their interaction on the neural response to outcome processing, we approached this question differently from former studies, many of which used difference waves (Glazer and Nusslock, 2021; Hajcak et al., 2007; Holroyd et al., 2008; Holroyd and Coles, 2002; Holroyd and Krigolson, 2007; Talmi et al., 2013; van Boxtel, 2004; Walsh and Anderson, 2012). In the present study, we aimed at giving a holistic perspective on feedback processing. As noted above, previous work has hinted that both surprise and valence contribute to feedback related EEG dynamics, but the precise nature of their interaction remains elusive. Here, we leveraged single trial regression and the power of a large sample to parse out the contributions of these factors on the EEG signal. While we have previously used instrumental learning tasks (Burnside et al., 2019; Fischer and Ullsperger, 2013; Kirschner et al., 2021), we exclude this learning aspect here. Moreover, when we use the term “FRN” in the context of the present work, we mean modulations of the EEG signal in a latency range of 200 to 300 ms over frontocentral regions, and do not refer to any particular ERP quantification.

Our goal was to differentiate changes of the FRN amplitude and the P3 complex as a function of valence and expectedness within a large sample. We therefore systematically manipulated valence and expectedness of the outcome to investigate the influence on the neuronal signal with the help of a single-trial regression approach. Feedback valence was either positive or negative. Outcome expectedness was conceptualized as global surprise. Here, the level of task difficulty was manipulated between blocks by increasing the expectancy of positive feedback or increasing the expectancy of negative feedback without the subjects’ knowledge. Additionally, we investigated local surprise by examining the influence of the recent trial history on the feedback-locked neuronal signal. If the FRN reflects mere surprise, a response to salience in the form of an unsigned RPE, the component should be insensitive to valence. Therefore, a component within the timeframe of the FRN should show no main effect of valence and no interaction of expectedness and valence, but a strong main effect of unsigned RPE size involving outcome probability (Sambrook and Goslin, 2015). In consequence, the FRN should be equally large for worse-than-expected and better-than-expected outcomes (Walentowska et al., 2019). Contrarily, if the FRN encodes signed RPEs, we would expect a valence x expectedness interaction, where the FRN for unexpected events differs between worse-than-expected and better-than-expected events. A sole main effect of valence would mean that the FRN represents the outcome itself and does not encode any RPE. Two non-interacting main effects of valence and expectedness would indicate two independent processes influencing the neuronal signal in the FRN latency range. Hypotheses are visualized in Fig. 1C. Concerning the P3 complex, we expect a clear effect of expectedness: unexpected outcomes should induce a larger P3b than expected outcomes.

To elaborate on the topic of behavioral adaptations following feedback, we used an advanced measure of change in response time between two consecutive trials, which reflects improvement or deterioration in task performance from one trial to the next. Since previous research has found that the type and expectedness of feedback could affect the extent of adaptation and that this adaptation has correlates in the neuronal signal (Holroyd and Krigolson, 2007), we considered the influence of the change in response time on the neuronal signal as a function of the valence and expectedness of the feedback. Specifically, we expected larger adaptations after negative feedback. Exploratorily, this adaptation could be affected by outcome expectancies, whereby unexpected negative feedback should be accompanied by larger and expected negative feedback by smaller behavioral adjustments.

2. Methods

2.1. Participants

1000 young, healthy participants were recruited at the Radboud University of Nijmegen, Netherlands (388 datasets; 03/2011–06/2011) and at the Max Planck Institute for Human Cognitive and Brain Sciences in Leipzig, Germany (all remaining; 05/2012–03/2016). Screened via interview, exclusion criteria were: any present or past psychiatric or neurological disorders, regular use of medication, drug abuse, alcohol intake at day of study. 8 subjects had to be excluded due to recording failures or

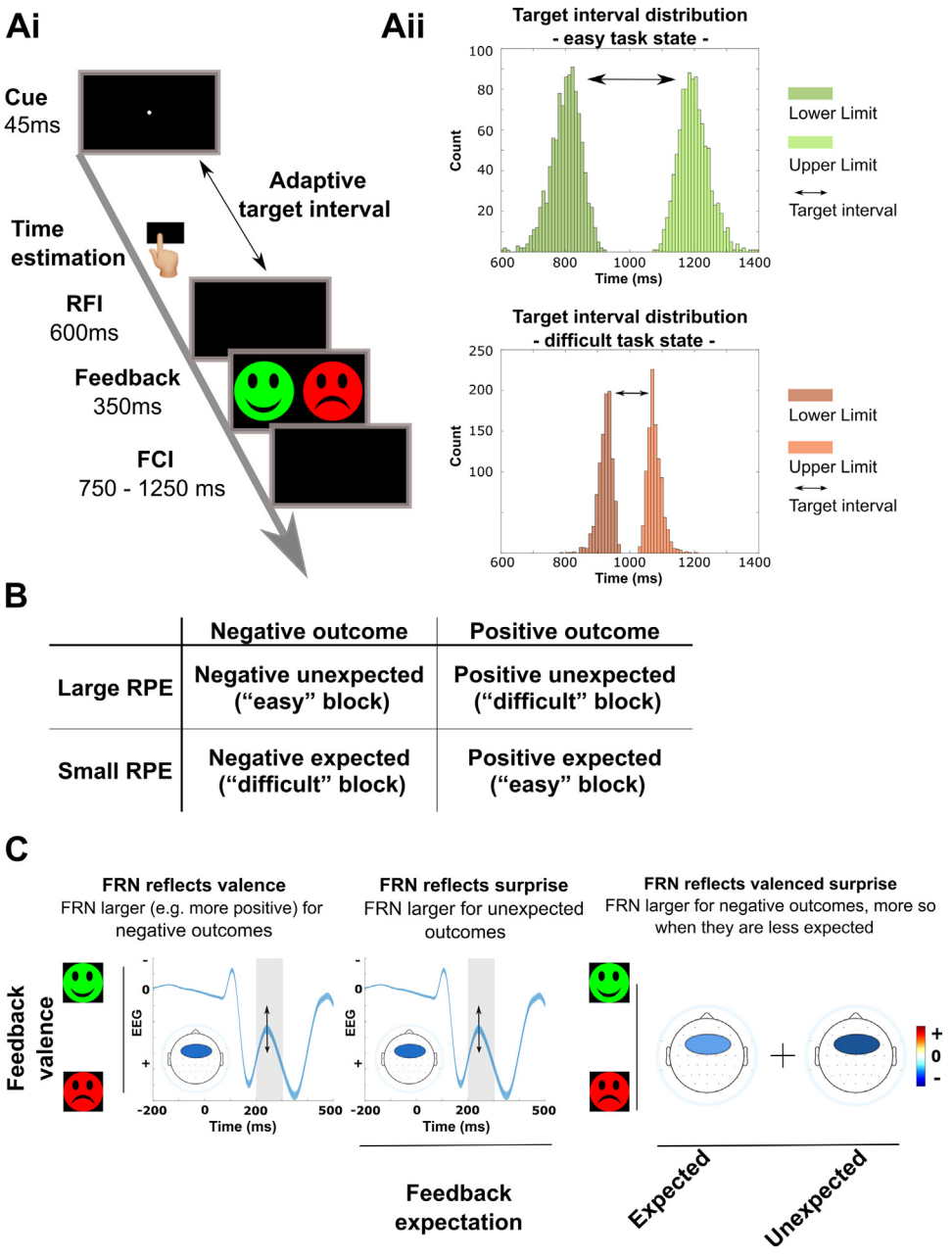

Fig. 1. Illustration of the task design and theoretical hypotheses on task factors on the FRN signal. (**Ai**) Timeline of a single trial. Each trial starts with a cue represented by a fixation cross. From cue onset on, participants are instructed to estimate one second and to indicate the end of the estimated time interval by button press. The time window for a correct response is adaptive and differs between conditions (control, easy, difficult). A reaction feedback interval (RFI) of 600 ms follows the response. Participants then receive either positive or negative feedback in the form of a green smiley for correct response and a red frowny for incorrect response, which is displayed for 350 ms. This is followed by a variable feedback cue interval (FCI) of 750–1250 ms before the next trial starts. (**Aii**) Target interval distributions for the different task states (easy and difficult). (**B**) Experimental conditions and their respective correspondences to a reward prediction error (RPE) as a function of the valence of the feedback. (**C**) Illustration of theoretical hypotheses for FRN signals. Left: FRN reflects valence. FRN is larger (e.g., more negative) on all negative outcomes. When comparing positive vs. negative feedback, this should be reflected in frontocentral negativity as depicted in the respective topography plot. Middle: If the FRN is reflecting mere surprise, the FRN should be larger for unexpected feedback (positive outcomes in the difficult task state and negative outcomes in the easy task state). Right: The FRN reflects "valenced surprise" (e.g., prediction errors). Larger FRN in negative outcomes (reflected in a frontocentral negativity), more so when they are less expected than when they are common.

poor data quality (see 2.3 for details). The sample consists of 493 female and 499 male subjects between 18 - 40 years ($M = 24.22$; $SD = 4.03$). The majority of the participants were right-handed ($N = 914$), 44 were left-handed, and 33 ambidextrous or retrained (1 not reported). The study was approved by the Institutional Review Board/Ethics Committee of the Radboud University of Nijmegen (ECG04032011) and the University of Leipzig (285-09-141209) and written informed consent was obtained from all participants after briefing prior to study enrolment. The study was conducted in accordance with the Declaration of Helsinki.

2.2. Experimental paradigm

We used a modified version of a time estimation task, where the participants had to estimate the duration of one second by keystroke with a fixation cross as onset time point (Gruendler et al., 2011; Holroyd and Krigolson, 2007, see Fig. 1Ai). Positive Feedback for a correct response (i.e. responding in a time window of 1000 ms ± 100 ms initially) was given in form of a green smiley, negative feedback for an incorrect response was visualized with a red frowny. Within the experiment, every subject underwent three conditions, where the time window (TW) for correct responses was adapted differently such that negative feedback was more likely than positive feedback ("difficult"), negative and positive feedback were equally likely ("control"), and negative feedback was less likely than positive feedback ("easy"), respectively. Within the control condition, the TW for positive feedback increased by 10 ms on error trials and decreased by 10 ms on correct trials symmetrically. In the easy condition, the window size increased by 12 ms on error trials and decreased by 4 ms on correct trials. In the difficult condition, adaptation reversed compared to the easy condition, so that the TW narrowed faster on correct responses (−12 ms) than it grew after incorrect responses (+4 ms; see Fig. 1Aii). Participants always started with the control condition, where a TW for positive feedback was initialized at 1000 ms ± 100 ms (positive feedback was given when the response fell between 900 and 1100 ms). They then continued with either the easy

or the difficult condition and went through each condition once, counterbalanced over participants. The time window to start with in the first trial of a new block was equal to the time window resulting from the last trial of the preceding block. The control condition only served to intercept initial adaptation processes and to define the initial time window and was therefore not equivalent to the other conditions, which is why it was excluded from analysis. The task consists of 450 trials in total, 50 trials in the control condition, 200 trials each in the difficult and easy conditions. The inter-trial interval (feedback-cue interval, FCI) varied between 750 ms and 1250 ms. Fig. 1B shows the conceptual mapping of the task blocks (easy/difficult) to the associated size of the RPE and the valence of the outcome.

2.3. EEG acquisition and processing

Electroencephalic signals were continuously recorded at 500 Hz sampling rate with BrainAmp MR plus amplifiers (Brain Products) from 64 Ag/AgCl sintered electrodes, which were mounted in an elastic cap according to the extended 10–20 system with impedances kept below 5kΩ. The ground electrode was placed at the sternum. Electrodes to capture horizontal and vertical eye movements were mounted next to both eyes and above and below the left eye. The signal was online referenced to A1 (left mastoid). The recorded data was high (0.5 Hz) - and low (30 Hz) -pass filtered, re-referenced to common average, and epoched from -400 ms to 1500 ms locked to feedback onset. Artifactual epochs were automatically rejected based on signal outliers. Epochs that deviate over 5 SD from the mean probability distribution of the EEG signal were excluded (Delorme et al., 2007). We specified that a minimum of 10 trials but no more than 10% of the trials (N = max. 45) should be rejected. Therefore, the initial threshold of 5 SD was adaptively increased or decreased with a step size of 0.1 SD. This resulted in an average rejection of 20 epochs across all participants (range N = 10–44). Epochs were then demeaned and submitted to adaptive mixture independent component analysis (AMICA, Palmer et al., 2012). Independent components including artifactual signals (i.e. eye blinks) were rejected with the help of sample-based ratings of two EEG-experienced researchers in combination with a correlation-based approach (inspired by the Corrmap approach; Viola et al., 2009). A baseline of − 350 ms until 0 ms prior to feedback onset was used. The data was then analyzed with multiple robust single-trial regression analyses (see Fischer and Ullsperger, 2013 for details). EEG datasets for which ICA did not converge or too less trials for specific regressors existed were excluded (8 subjects), resulting in a final sample of 992 participants. For EEG and behavioral analysis, EEGLab 13.5 toolbox (Delorme and Makeig, 2004) and customized code written in MATLAB R2019b version 9.7.0.1190202 (MathWorks) was used.

2.4. Data analysis

2.4.1. Behavioral analyses

Data for building behavioral regressors were either directly derived from the behavioral data or, in some cases, calculated from combinations of other behavioral variables. *Valence* (Val) represents the qualitative direction of the feedback, either positive (=0) or negative (=1). The regressor *expectedness* (Exp) is a dichotomous variable, where unexpected events (=0) indicate trials with negative feedback during the easy condition and trials with positive feedback during the difficult condition. Expected events (=1) are coded vice versa (positive feedback in easy condition; negative feedback in difficult condition). *Reaction time* (RT) reflects the absolute reaction time from fixation cross onset until button press. The following variables reflect local surprise: the *number of trials since the last negative or positive event* (TrialsSinceNeg/Pos) indicates how long ago the last event of the same valence occurred. The longer it has been, the bigger the local surprise. For these two variables, corresponding trials are cumulated separately for negative and positive events. In addition, if participants build up an internal representation of the target time, another form of local surprise can be conceptualized as the absolute difference between 1000 ms (the target time) and trial-based reaction time. This variable is represented by the parametric regressor *reaction time deviation* (RT_dev; unsigned). The closer the participant is to 1000 ms and still receives negative feedback, the bigger the local surprise. *Reaction time change* (RT_change) was calculated (Eq. (1)) by subtracting the absolute reaction time difference of the following trial from the absolute reaction time difference of the current trial and therefore, represents a measure of performance adaptation. The results of this calculation (see Eq. (1)) could either take on positive values, which represent performance improvement (i.e. coming closer to 1000 ms), or negative values, which represent performance deterioration (increasing distance to 1000 ms):

$$RT\_change = \left|\left(RT_{current\ trial} - 1000ms\right)\right| - \left|\left(RT_{following\ trial} - 1000ms\right)\right| \quad (1)$$

As noise regressors without interest, logarithm of the trial number in the current block (BlockTr) and inter-trial interval (FCI) were included in all regression models. The parameters BlockTr, FCI, RT, RT_dev, TrialsSinceNeg/Pos, and RT_change were z-standardised.

We calculated a robust multiple regression with behavioral adjustment (absolute difference between two consecutive trials in ms) as the outcome. Valence, expectedness, their interaction, as well as BlockTr and FCI served as predictors:

$$Behavioral\ adjustment = \beta_0 + \beta_1 \times Val + \beta_2 \times Exp + \beta_3 \times BlockTr + \beta_4 \times FCI + \beta_5 \times Val \times Exp + \varepsilon \quad (2)$$

2.4.2. Grand averages

We calculated grand average ERPs at two electrodes for crossed conditions (negative feedback-expected; negative feedback-unexpected; positive feedback-expected; positive feedback-unexpected) by averaging across all subjects. The site of maximal FRN activity is, according to the literature (Williams et al., 2020), electrode FCz and the site of maximal P3b activity is, according to the literature (Intriligator and Polich, 1994; Polich, 2007), electrode Pz. Therefore, we chose FCz and Pz to visualize the neuronal signal depending on feedback.

2.4.3. Single-trial EEG analyses

We furthermore employed several multiple robust regressions, within (1st level) and across subjects (2nd level; Fischer et al., 2016; Fischer and Ullsperger, 2013). General linear models (GLM) were built to regress single-trial EEG activity at each electrode and time point against behavioral parameters. The regressions were performed on 59 electrodes in a time window from −200 ms to 1000 ms, feedback-locked. The output of these analyses was in the form of regression coefficients revealing the time course and scalp topographies of the relationship between each predictor and neuronal activity. Standardized beta-values can be tested via two-tailed one-sample t-tests, which were done separately at each data point in a whole-brain approach across subjects. To account for multiple comparisons, p-values within one model were corrected using false discovery rate (FDR). Trials of the control condition were excluded from regression analyses.

Within the first GLM (1a), we were interested in the influences of valence of feedback, expectedness, and the interaction of both on the neuronal signal:

$$\text{(GLM 1a)}: EEG\ amplitude = \beta_0 + \beta_1 \times Val + \beta_2 \times Exp + \beta_3 \times BlockTr + \beta_4 \times FCI + \beta_5 \times Val \times Exp + \varepsilon \quad (3)$$

To further disentangle the results revealed in the first GLM, we split the data in expected and unexpected trials within a subordinate GLM

(1b). This enables us to have a more detailed look on the effect of valence comparing negative- and positive-feedback-trials for expected and unexpected trials separately:

$$(\text{GLM 1b}): EEG\ amplitude = \beta_0 + \beta_1 \times Val + \beta_2 \times BlockTr + \beta_3 \times FCI + \varepsilon \quad (4)$$

(ran separately for expected and unexpected outcomes)

By building a second main GLM and splitting the data in positive- and negative-feedback trials, it was possible to resolve the interaction between valence and expectedness and to further investigate the differential effects of expectedness or global surprise, respectively. Additionally, we included further variables, which give information on local surprise, like TrialsSinceNeg/Pos and RT_dev:

$$(\text{GLM 2}): EEG\ amplitude = \beta_0 + \beta_1 \times Exp + \beta_2 \times RT + \beta_3 \times TrialsSinceNeg/Pos + \beta_4 \times RT\_dev + \beta_5 \times BlockTr + \beta_6 \times FCI + \varepsilon \quad (5)$$

(ran separately for trials with negative and positive feedback)

In the last GLM 3, we were interested in the neuronal signal changes due to performance adaptation. Therefore, we created main GLM 3a including the regressor RT_change, which reflects performance improvement or deterioration between the current and the consecutive trial. The interaction of feedback valence and RT_change served as a predictor as well (Eq. (6)). In a subordinate GLM 3b, we disentangled this interaction by running separate regressions for trials with negative and positive feedback (Eq. (7)). Because the participants tend to adjust their RT more after negative feedback, we calculated another subordinate GLM 3c for negative-feedback trials to examine the interaction between expectedness and behavioral adaptation exploratorily (Eq. (8)).

$$(\text{GLM 3a}): EEG\ amplitude = \beta_0 + \beta_1 \times Val + \beta_2 \times RT\_change + \beta_3 \times Exp + \beta_4 \times BlockTr + \beta_5 \times FCI + \beta_6 \times Val \times RT\_change + \varepsilon \quad (6)$$

$$(\text{GLM 3b}): EEG\ amplitude = \beta_0 + \beta_1 \times RT\_change + \beta_2 \times Exp + \beta_3 \times BlockTr + \beta_4 \times FCI + \varepsilon \quad (7)$$

(ran separately for trials with negative and positive feedback)

$$(\text{GLM 3c}): EEG\ amplitude = \beta_0 + \beta_1 \times RT\_change + \beta_2 \times Exp + \beta_3 \times BlockTr + \beta_4 \times FCI + \beta_5 \times Exp \times RT\_change + \varepsilon \quad (8)$$

(ran for trials with negative feedback)

We were particularly interested in beta-value peaks approximately in the latency ranges (FRN: 200–300 ms; P3a/P3b: 300–600 ms; P3a usually earlier) and topographic locations (FRN/P3a: frontocentral; P3b: centroparietal) of FRN, P3a and P3b as reported in the literature (Polich, 2007; Sambrook and Goslin, 2015; San Martín, 2012; Ullsperger et al., 2014b), because these are components that typically occur following feedback. Thus, for post-hoc t-tests after regression analysis, we derived latencies of local beta-value peaks of the predictors in FRN- or P3-time windows based on visual inspection and comparing with the respective ERP. Individual beta-value peak time points (not all shown in Fig. 4) were extended by including beta-values in a time window of ±20 ms around the peak and using the average of them. The indicated electrodes usually include the electrode with the strongest effect, otherwise they represent strong local effects.

3. Results

3.1. Behavioral results

Overall, the participants performed well in the task, the mean reaction time across all conditions was 1032.10 ms ± 218.21 ms (see Fig. 2A). Manipulation of difficulty by different task states was successful: within the easy condition, participants received positive feedback in 70.27% (SD_{easy} = 3.98%) of the trials, while in the difficult condition, only 29.62% ($SD_{difficult}$ = 2.50%; $M_{control}$ = 41.70%; $SD_{control}$ = 8.18%) of the trials were followed by positive feedback (see Fig. 2B).

In Fig. 2D, the absolute frequencies of averaged reaction time changes after negative/positive feedback (Di) and after expected/unexpected feedback (Dii) overall participants can be seen. Behavioral adjustments after negative feedback are bigger (M_{neg}= 230.39 ms; M_{pos}= 145.06 ms; $t(1982) = -42$, $p < 0.001$, $d = 1.89$) and within-subject more widely distributed (SD_{neg}= 180.20 ms; SD_{pos}= 120.68 ms; $t(1982) = -37$, $p < 0.001$, $d = 1.68$) than after positive feedback. Adjustments differ slightly with bigger adjustments and wider distributions within-subject for unexpected events (M_{unexp}= 197.52 ms; M_{exp}= 180.53 ms; $t(1982) = -8$, $p < 0.001$, $d = 0.36$; SD_{unexp}= 163.85 ms; SD_{exp}= 152.02 ms; $t(1982) = -7$, $p < 0.001$, $d = 0.29$). These results indicate that feedback valence and expectedness differentially affect subsequent behavior. To parse behavioral adjustments at finer levels of detail, we analyzed behavioral adjustments using multiple robust regression (see Fig. 2C). Predictors included expectedness (expected vs. unexpected feedback), valence (positive vs. negative feedback), and the interaction between these factors. In addition, we included FCI and trial number as regressors of no interest. The results confirmed a main effect of expectedness (mean $t = 0.10$, $t(991) = 2.62$, $p < 0.05$ (bonf cor), $d = 0.08$, 95% CI [0.02, 0.17]) and valence (mean $t = 3.89$, $t(990) = 74.18$, $p < 0.001$ (bonf cor), $d = 2.36$, 95% CI [3.79, 4.00]; Fig. 2Ci). Critically, the interaction between expectedness and valence showed that behavioral adaptations after negative feedback were larger, when negative feedback was less expected (mean $t = -1.17$, $t(990) = -18.65$, $p < 0.001$ (bonf cor), $d = -0.59$, 95% CI [−1.29, −1.05]; Fig. 2Cii). This may suggest, that participants adjust their behavior more after negative feedback during broader target windows. In contrast, they adjusted their behavior after negative feedback less, when the target window was narrow (i.e., during the difficult task state). In other words, surprise had a reinforcing effect on behavioral adjustments when feedback was negative. We took this as motivation for further analyses trying to disentangle the differential influences of valence and expectedness on behavior and EEG correlates. As the absolute change in RT between two consecutive trials does not allow direct evaluation of the adaptivity of the behavioral adjustment, we calculated the variable RT_change as a measure of performance adaptation for subsequent analyses investigating the association between feedback-related behavioral adaptions and EEG activity.

3.2. Electrophysiological results

3.2.1. Event-related potentials

To gain a first impression of the EEG-data and to see, whether or not our paradigm evokes the expected ERP results, we show the averaged ERP waves for the crossed conditions, expected/negative, unexpected/negative, expected/positive, and unexpected/positive for two electrodes, FCz and Pz (see Fig. 3). At FCz (Fig. 3Ai), the amplitude during the time window of the FRN seems to be more pronounced when participants received negative (yellow and red) rather than positive feedback. When rewards were less expected (green line), the FRN signal was more positive than in the other condition (expected rewards, blue line), whereas the FRN on negative trials was similar for expected (yellow) and unexpected (red) feedback. The amplitude during the time window of the P3b component seems larger for unexpected events (green and red) than for expected events (blue and yellow). Visually comparing un-

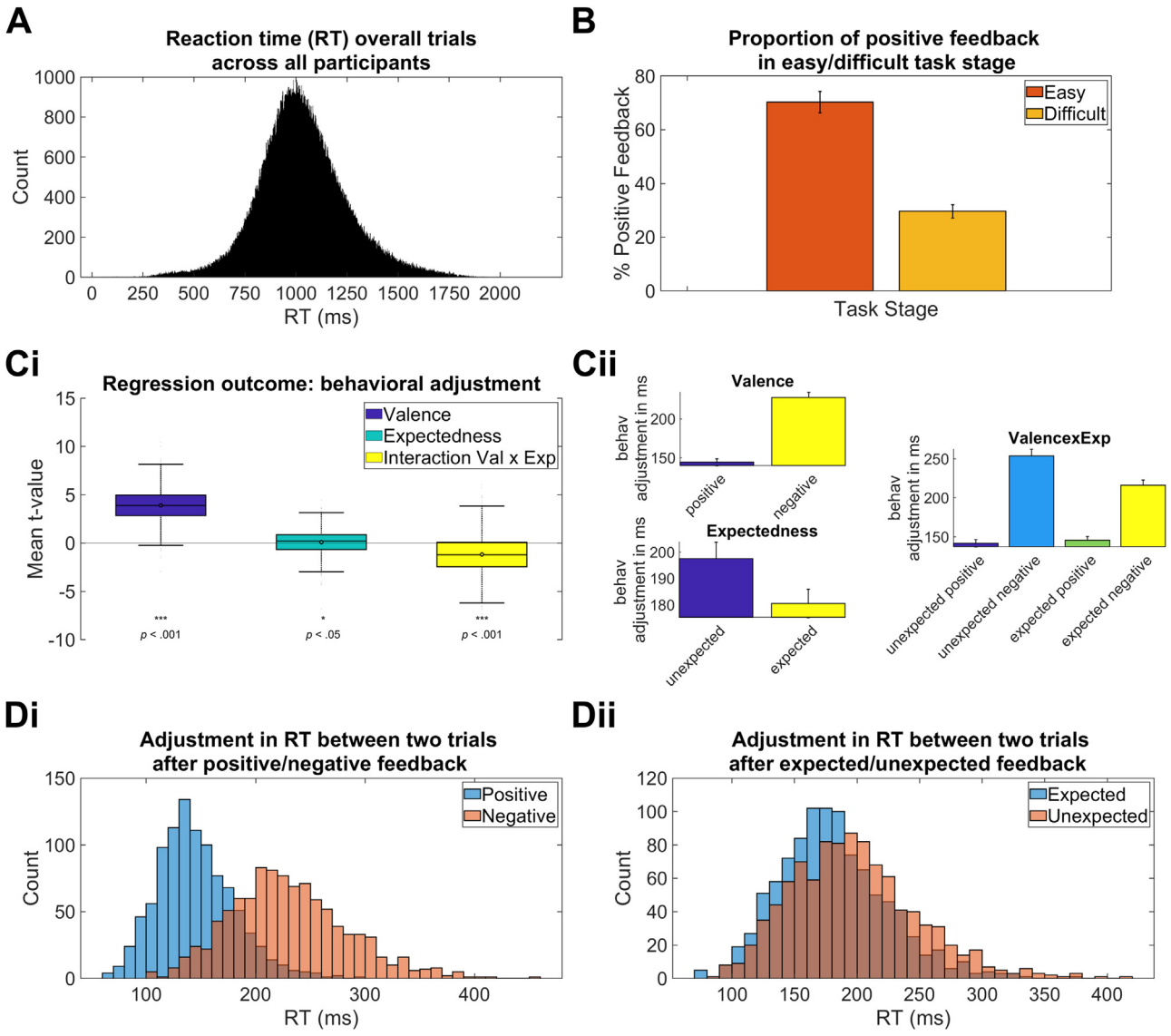

Fig. 2. Frequencies of reaction times and behavioral adjustments and influencing factors. (**A**) Frequencies of response times (in ms) of all trials across all participants. (**B**) shows the percentage of positive feedback received for both conditions across all participants. The dark orange box represents the easy condition and light orange the difficult condition. (**Ci**) Multiple robust regression with behavioral adjustment from current to the consecutive trial (change in reaction times in ms) as outcome. Valence, expectedness, and their interaction significantly predict behavioral adjustment. To correct for multiple comparisons Bonferroni correction was used. (**Cii**) Unexpected negative feedback elicits the largest behavioral adjustment. (**Di**) Frequencies of absolute behavioral adjustment from current to the consecutive trial (change in reaction times in ms) after negative (red color bars) and positive feedback (blue color bars). (**Dii**) Frequencies of behavioral adjustment (change in reaction time in ms) after unexpected (red) and expected (blue) feedback.

expected negative (red) and unexpected positive feedback (green) in the time window of the P3 complex, P3 amplitude seems to be affected by valence as well, as negative feedback increases the amplitude.

The EEG data in the time window of the P3 complex looks slightly different at electrode Pz (Fig. 3Bi) compared to FCz. The waveforms start do differ at around 200 ms after feedback onset. Unexpected positive feedback (green) seems to be associated with the most positive signal from 220 ms on. Nevertheless, the grand average ERP approach does not allow a temporally and spatially accurate determination of independent contributions to the neuronal signal: to investigate when and where which factors influence the neuronal signal and how they interact, it is essential to use other methods. The beta-value courses of the main predictors (Fig. 3Aii; Bii) are described in the context of the regression analysis (see 3.2.2).

The visual inspection of the grand average EEG activity supported our initial hypotheses concerning the influence of expectedness, valence, and their interaction on the feedback-locked EEG signal. For rigorous statistical testing and in order to disentangle this modulation of the signal temporally and spatially, and in dependence of possible confounding factors, we applied a multiple robust single-trial regressions approach (Fischer et al., 2016; Fischer and Ullsperger, 2013).

3.2.2. *Modulation of EEG signal by valence and expectedness of feedback*

GLM 1a examined the effects of feedback *valence, expectedness*, and their *interaction* on neuronal EEG activity (Fig. 3Aii, Bii and Fig. 4 row 1–3). From approximately 130 ms until 300 ms, there was a sustained negative effect of the *valence* regressor, that spanned over frontocentral electrode sites (Fig. 3Aii; Fig. 4, row 1, shown from 200 ms onwards). Thus, EEG amplitudes were more negative following negative feedback (most pronounced at FCz, peak @ 250 ms, $b = -2.63$, $t(991) = -48.10$, $p = 1.81\times10^{-261}$, $d = -1.52$, 99% CI [−2.74 −2.53], *crit* $p = 0.035$), which indicates that valence coding is present in the typical latency range and topography of the FRN. Furthermore, there is another valence-specific but more parietal negative effect starting at 260 ms un-

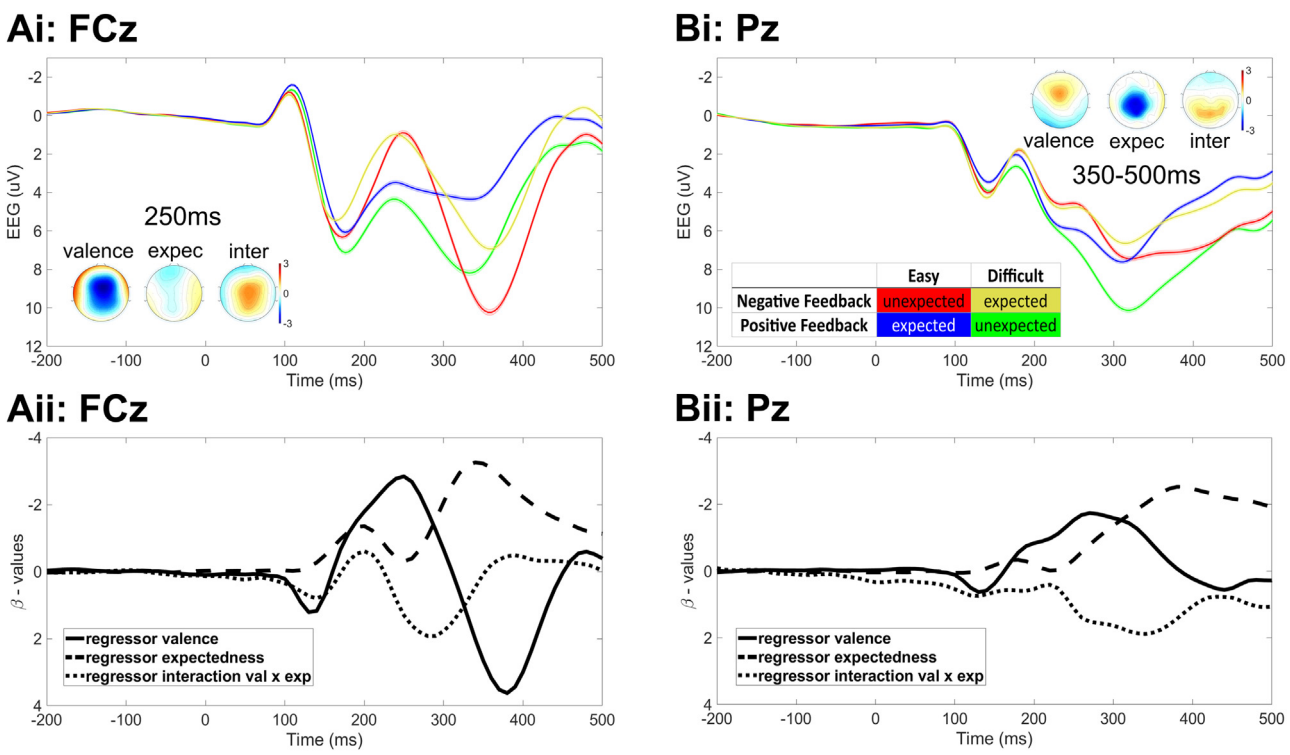

Fig. 3. Grand average feedback-locked ERPs of the crossed conditions and beta-value courses of the main regressors in GLM 1a. (**Ai**) The averaged feedback-locked ERPs across participants at electrode FCz. The table in (Bi) shows the task design including the matrix of different task stages. Different colors represent the crossed conditions: expected negative feedback (yellow); unexpected negative (red); expected positive feedback (blue); unexpected positive feedback (green). Shades represent SEM (very small and therefore barely visible). Regression weight topographies of the regressors valence, expectedness, and their interaction are shown at 250 ms after feedback. (**Aii**) The course of the beta-values from GLM1a of the regressors valence, expectedness, and their interaction at FCz are shown below. (**Bi**) The averaged feedback-locked ERPs across participants at electrode Pz. Regression weight topographies of the regressors valence, expectedness, and their interaction averaged across latencies from 350 to 500 ms after feedback are shown. Regression weights in the topoplots are fdr (false discovery rate)-corrected and nonsignificant electrodes are masked in white. (**Bii**) The course of the beta-values from GLM1a of the regressors valence, expectedness, and their interaction at Pz are shown below.

til 340 ms (Fig. 3Bii; Fig. 4 row 1). This negative covariation was followed by a frontocentral positive covariation between 320 and 480 ms (most pronounced at FCz, peak @ 380 ms, b = 3.35, $t(991)$ = 46.44, $p = 6.47\times10^{-251}$, d = 1.48, 99% CI [3.21 3.49], *crit* p = 0.035; see Fig. 4, row 1). Topography and latency suggest that it is a major contributor to the P3a.

Within GLM 1a, we also tested the influence of *expectedness* on the EEG signal. This regressor shows a sustained and spatially broader fronto-centro-parietal effect on the P2/P3 complex between 240 and 530 ms (most pronounced at Cz, peak @ 350 ms, b = −3.26, $t(991)$ = −60.32, p < 0.0001, d = −1.92, 99% CI [−3.37, −3.15], *crit* p: 0.0001; see Fig. 4, row 2). The signal is more positive for unexpected compared to expected outcomes. However, the effect of expectedness prior to 240 ms seems to be less pronounced and more frontally distributed (Cz, smaller peak @ 190 ms, b = −0.91, $t(991)$ = −34.42, $p = 1.93\times10^{-171}$, d = −1.09, 99% CI [−0.96, −0.86], *crit* p = 0.0001). Taken together, the FRN amplitude is influenced by valence, but is less affected by expectedness (between 200 and 300 ms; $mean_{val}$ = −0.21 ± 0.004 vs. m_{exp} = −0.03 ± 0.003; $t(991)$ = −41.46, $p = 1.14\times10^{-218}$, d = 1.82). Valence *and* expectedness (i.e. global surprise, resp.) seem to influence the P2/P3 complex. Whereas the valence effect appears to be frontocentral, violation of expectedness shows a broader effect from frontocentral to parietal areas.

Additionally, we were interested in whether and how both regressors interact with each other as an interaction would be predicted for an RPE signal. Derived from the course of beta-values, from approximately 230 ms on, the *valence* x *expectedness* regressor covaried positively with the neuronal activity (FCz, peak @ 280 ms, b = 1.81, $t(991)$ = 17.10, $p = 1.28\times10^{-57}$, d = 0.54, 99% CI [1.60, 2.01], *crit* p = 0.032; see Fig. 4, row 3). By visual inspection, this broad frontocentral positive covariation extends to parietal areas over time. To summarize, the interaction of valence and expectedness shows a strong significant effect during the FRN latency range for both the early FRN-peak and for the later part of the FRN on fronto-centro-parietal electrodes. This underlines that the FRN encodes an RPE signal. To disentangle the interaction between valence and expectedness, we conducted separate regression models by splitting the data in expected and unexpected trials (GLM 1b).

In GLM 1b, we found a negative covariation of *valence* with the neuronal signal from 160 ms to 310 ms in both, unexpected (FCz, peak @ 260 ms, b = −3.55, $t(991)$ = −41.95, $p = 6.64\times10^{-222}$, d = −1.33, 99% CI [−3.72, −3.39], *crit* p = 0.036; see Fig. 4, row 5) and expected trials (FCz, peak @ 240 ms, b = −2.41, $t(991)$ = −37.89, $p = 6.14\times10^{-195}$, d = −1.20, 99% CI [−2.53, −2.28], *crit* p = 0.033; see Fig. 4, row 4). Comparing the regression weights at their respective peaks, the valence effect during the time window of the FRN is more pronounced in unexpected trials (m_{unexp} = −3.55 ± 0.08 vs. m_{exp} = −2.41 ± 0.06; $t(991)$ = −11.49, $p = 8.63\times10^{-29}$, d = 0.5). To formally test for spatiotemporal differences of valence coding between expected and unexpected feedback in the FRN time window, we extracted averaged b-values at FCz and Pz and at the latencies 200 ms (± 20 ms) and 260 ms (± 20 ms) from the valence regressor of the respective GLM 1b. These data were then analyzed in a three-way ANOVA with the factors latency, location, and expectedness. Results show a significant three-way interaction of expectedness x location x latency ($F(1991)$ = 122.39, p < 0.001, η^2 = 0.11) indicating that for expected events, valence is coded earlier (200 ms) and more frontally (FCz), whereas for unexpected events, valence is processed later (260 ms) and with parietal involvement (Pz).

Afterwards, until approximately 450 ms, the signal covaries positively with *valence* in both, unexpected (FCz, peak @ 380 ms, b = 3.57, $t(991)$ = 30.53, $p = 8.39\times10^{-145}$, d = 0.97, 99% CI [3.34, 3.80], *crit*

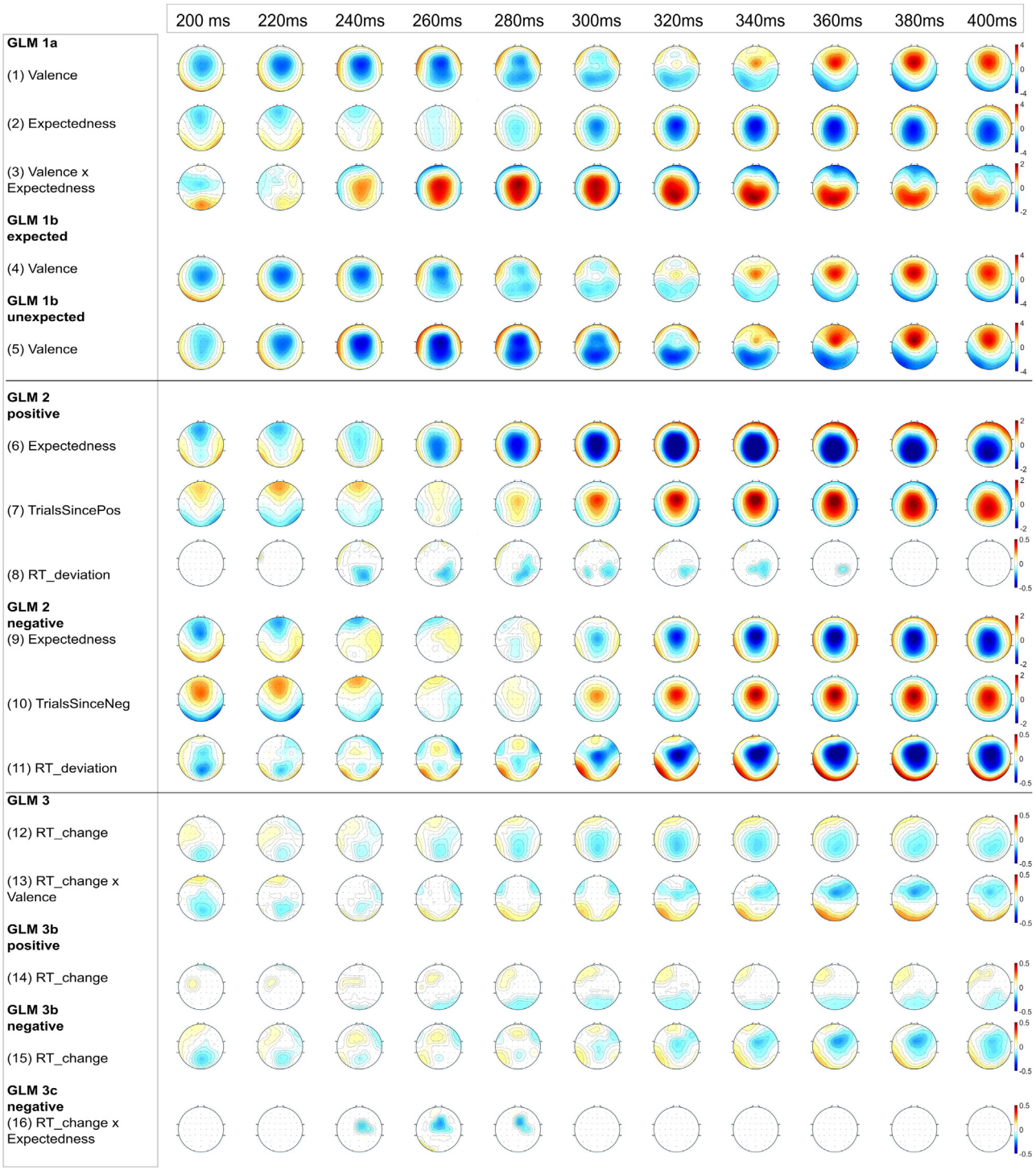

Fig. 4. Multiple single-trial robust regression results for feedback-locked epochs. Feedback-locked regression weight (beta) topographies in 20 ms time steps spanning from 200 ms to 400 ms are shown. The corresponding GLM and predictors are listed on the left. Blue colors are associated with negative covariations, red colors with positive covariations. Interpretation of the polarity depends on the coding of the predictor (see methods Section 2.4.1). Scaling can be seen on the right and differs between regressors. For corrections of multiple comparisons, false discovery rate (FDR) was used. Nonsignificant data points are masked in white.

$p = 0.036$; see Fig. 4, row 5) and expected trials (FCz, peak @ 380 ms, $b = 3.27$, $t(991) = 41.67$, $p = 4.33\times10^{-220}$, $d = 1.32$, 99% CI [3.11, 3.42], *crit* $p = 0.033$; see Fig. 4, row 4). Comparing the regression weights at their peak at 380 ms, the effect is more pronounced in unexpected trials compared to expected trials ($m_{unexp} = 3.57 \pm 0.12$ vs. $m_{exp} = 3.27 \pm 0.08$; $t(991) = 2.40$, $p = 0.02$, $d = 0.10$). This result illustrates the involvement of surprise: if the event is unexpected, the positive-going valence effect on the P3b is stronger.

Taken together results from GLM 1b, aiming to disentangle the interaction of valence and expectedness of feedback, we found an effect of valence on the neuronal signal during the time windows of the FRN and the P3 for expected *and* unexpected events. In both, the time win-

dow of the FRN and the P3, the effect of feedback valence was more pronounced in unexpected events.

To *directly* compare the neuronal activity of expected and unexpected events in dependence of valence, we conducted GLM 2 on positive- and negative feedback trials separately. As can be seen in Fig. 4, row 6, there was an influence of expectedness for positive-feedback trials at frontal and frontocentral electrodes starting before the FRN (90 ms; FCz, peak @ 160 ms, $b = -0.56$, $t(991) = -11.75$, $p = 6.10\times10^{-30}$, $d = -0.37$, 99% CI [−0.65, −0.47], *crit* $p = 0.029$; see Fig. 4, row 6) and spanning the entire FRN latency range. For negative-feedback trials, there is a small negative covariation of expectedness with the neuronal signal at frontal and frontocentral electrodes starting early around 160 ms (FCz, peak @ 200 ms, $b = -0.86$, $t(991) = -16.09$, $p = 6.47\times10^{-52}$, $d = -0.51$, 99% CI [−0.96, −0.75], *crit* $p = 0.027$; see Fig. 4, row 9). In contrast to the expectedness effect in positive-feedback trials, in negative-feedback trials there seems to be a weaker frontocentral effect in the second half of FRN latency ranges between 240 ms and 280 ms. In other words, for negative outcomes, the FRN is nearly unmodulated by expectedness. In contrast, for positive outcomes, the positive-going shift of the waveform is significantly pronounced when the outcome is unexpected. A stronger modulation on trials with positive feedback also applies to the later ERP components. During the time window of the P3, results show a significant negative covariation at central and centroparietal electrodes for the regressor expectedness for trials with positive feedback (Cz, peak @ 330 ms, $b = -2.49$, $t(991) = -34.73$, $p = 1.51\times10^{-173}$, $d = -1.10$, 99% CI [−2.63, −2.35], *crit* $p = 0.029$; see Fig. 4, row 6), but also for trials with negative feedback (FCz, peak @ 360 ms, $b = -2.06$, $t(991) = -22.04$, $p = 6.11\times10^{-88}$, $d = -0.70$, 99% CI [−2.25, −1.88], *crit* $p = 0.027$; see Fig. 4, row 9).

3.2.3. Modulation of EEG signal by local surprise

Next, we investigated neural coding of local surprise, that was reflected in two regressors within GLM 2, the *number of preceding trials since the last negative or positive trial appeared* and *reaction time deviation* from the target time of 1000 ms. The results indicate that the longer it has been since the current feedback was last seen (i.e., the bigger the local surprise), the more positive the P3b. On frontal electrodes, the first predictor covaried positively with the neuronal signal in both positive- (Fz, @ 220 ms, $b = 0.62$, $t(991) = 23.13$, $p = 5.57\times10^{-95}$, $d = 0.73$, 99% CI [0.56, 0.67], *crit* $p = 0.031$; see Fig. 4, row 7) and negative-feedback trials (Fz, @ 220 ms, $b = 0.82$, $t(991) = 30.43$, $p = 3.81\times10^{-144}$, $d = 0.97$, 99% CI [0.77, 0.88], *crit* $p = 0.033$; see Fig. 4, row 10). This effect is stronger in negative-feedback trials between 200 and 240 ms ($m_{pos} = 0.62 \pm 0.03$ vs. $m_{neg} = 0.82 \pm 0.03$; $t(991) = -5.71$, $p = 1.46\times10^{-8}$, $d = 0.25$). From 280 ms on, this predictor covaried positively with the neuronal signal in both positive- (FCz, peak @ 340 ms, $b = 2.07$, $t(991) = 43.49$, $p = 5.48\times10^{-232}$, $d = 1.38$, 99% CI [1.97, 2.16], *crit* $p = 0.031$; see Fig. 4, row 7) and negative-feedback trials (FCz, peak @ 360 ms, $b = 1.96$, $t(991) = 42.52$, $p = 1.19\times10^{-225}$, $d = 1.35$, 99% CI [1.87, 2.05], *crit* $p = 0.033$; see Fig. 4, row 10).

For the predictor *reaction time deviation* from the target time of 1000 ms, there is a negative covariation within the time frame of P3 only in negative trials (FCz, peak @ 370 ms, $b = -0.67$, $t(991) = -24.60$, $p = 1.19\times10^{-104}$, $d = -0.78$, 99% CI [−0.72, −0.62], *crit* $p = 0.023$; see Fig. 4, row 11). If the participant was close to 1 s, but negative feedback followed, subjective surprise might be enhanced and in consequence, P3 is more positive. This does not apply for the positive prediction error, considering only a small parietal to occipital activation can be found in positive-feedback trials between 240 and 340 ms (see Fig. 4, row 8). In conclusion, the present data (GLM 2) indicate that the P3 complex is driven by global *and* local surprise.

In GLM 2, we found that expectedness of feedback has only a small effect on the neuronal signal during the time window of the FRN. Meanwhile, global surprise during the P3 time window influences the neuronal signal in positive-feedback and negative-feedback trials. Furthermore, we found evidence for a positive covariation of local surprise and the P3.

3.2.4. Adaptation

We were interested in how the EEG signal, and especially, the FRN is associated with behavioral adaptations after making a false response. Therefore, we implemented another behavioral predictor in GLM 3, *reaction time change* (*RT_change*). It represents feedback adaptation in the consecutive trial, while positive values imply improvement (i.e. getting closer to 1 s) and negative values decline (further away from 1 s) in performance. Furthermore, we included the interaction of valence and adaptation, because we assume a stronger influence of adaptation after negative-feedback trials. Surprisingly, we only see a very small association between *RT_change* and the neuronal activity from 130 ms on (CPz, peak @ 220 ms, $b = -0.04$, $t(991) = -3.39$, $p = 0.001$, $d = -0.11$, 99% CI [−0.06, −0.02], *crit* $p = 0.047$; see Fig. 4, row 12). However, there is a negative covariation between *RT_change* at centroparietal electrodes (CPz, peak @ 320 ms, $b = -0.17$, $t(991) = -12.61$, $p = 6.36\times10^{-34}$, $d = -0.40$, 99% CI [−0.19, −0.14], *crit* $p = 0.047$; see Fig. 4, row 12) and the interaction of *feedback valence* x *RT_change* at frontal electrodes with the neuronal signal around 350 ms after feedback (FCz, peak @ 370 ms, $b = -0.22$, $t(991) = -7.58$, $p = 7.80\times10^{-14}$, $d = -0.24$, 99% CI [−0.28, −0.17], *crit* $p = 0.008$; see Fig. 4, row 13). These counter-intuitive findings imply that an improvement in the consecutive trial is associated with a smaller P3a amplitude. To disentangle the effects of the significant interaction between valence and behavioral adaptation, we split the data into negative- and positive-feedback-trials and used RT_change as a regressor of interest (GLM 3b). Within positive-feedback trials, RT_change does not seem to have a systematic influence on neuronal signals contributing to the FRN or P3 complex (see Fig. 4, row 14). For negative trials, there is a small negative covariation of RT_change with the neuronal signal at parietal electrodes in the time frame of the early FRN (Pz, @ 200 ms, $b = -0.15$, $t(991) = -10.88$, $p = 4.18\times10^{-26}$, $d = -0.35$, 99% CI [−0.18, −0.13], *crit* $p = 0.011$; see Fig. 4, row 15). Additionally, results show a negative covariation of RT_change with the neuronal signal in the time window of the P3 for negative-feedback trials (FC2, peak @ 360 ms, $b = -0.21$, $t(991) = -13.00$, $p = 8.59\times10^{-36}$, $d = -0.41$, 99% CI [−0.24, −0.18], *crit* $p = 0.011$; see Fig. 4, row 15). Because participants adjusted their behavior depending on the expectancy of negative feedback, we investigated the influence of the interaction of expectedness and RT_change after negative feedback on the neuronal signal in GLM 3c. Indeed, a frontoparietal negative covariation between 240 ms and 280 ms occurs in negative-feedback trials (FCz, peak @ 260 ms, $b = -0.19$, $t(991) = -4.99$, $p = 7.14\times10^{-7}$, $d = -0.16$, 99% CI [−0.27, −0.12], *crit* $p = 0.0004$; see Fig. 4, row 16).

4. Discussion

4.1. Factors influencing the early feedback-related neuronal signal

The current study found, based on a large sample of 992 participants, that valence and expectedness influence the neuronal signal and behavioral adjustments after feedback. Fig. 5 summarizes the contributions of feedback-related performance monitoring components to feedback-locked EEG dynamics in a schematic sketch. As can be seen, the effect of valence starts early around 180 ms at frontoparietal areas. Another negative covariation joins in from 260 ms on at centroparietal electrodes. This second, more parietal valence-specific effect was already reported in other studies (Gentsch et al., 2009; Ullsperger et al., 2014a) and appeared independently from frontocentral parts (Gentsch et al., 2009). Since the classification of the signal is still unclear, future research should address the origin of this phenomenon. With respect to global surprise or expectedness, we see a weaker frontal effect starting at an early latency even before 180 ms (see Fig. 5). The interaction of valence and surprise evokes a broad and sustained frontocentral effect from 230 ms on and it extends to parietal areas over time.

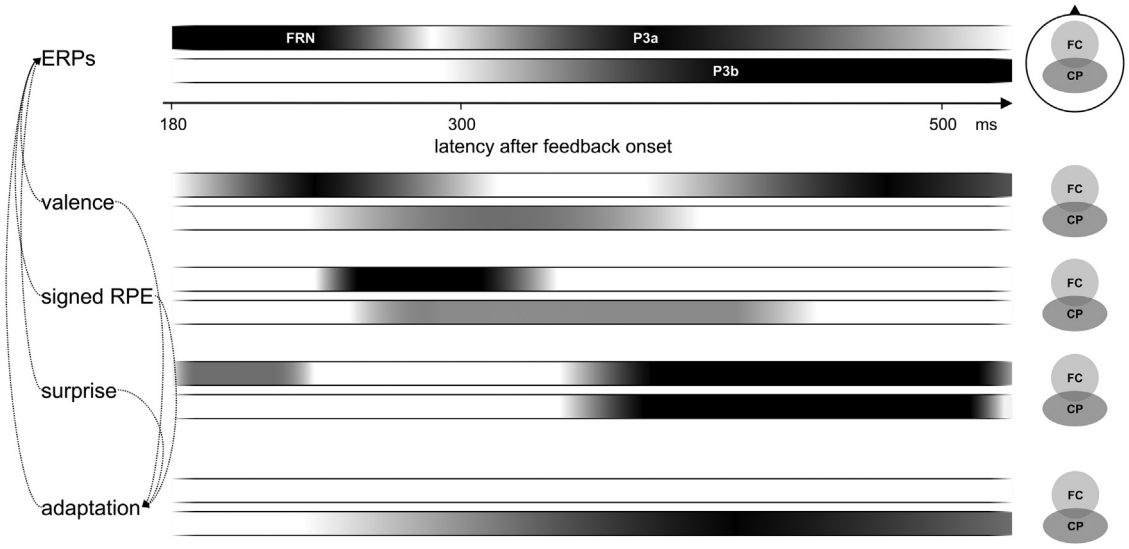

Fig. 5. Schematic representation of influencing factors and their manifestation in the neuronal signal and ERPs after feedback. ERP = event-related potential; FC = frontocentral; CP = centroparietal.

Negative feedback was associated with a sustained negativity in the FRN latency range. In the same time window, we found a negative covariation of the feedback-locked EEG activity for the expectedness regressor. These findings go in line with previous research (Holroyd and Krigolson, 2007) and support the RL-account in a way, that the FRN is not only driven by mere surprise. Moreover, we found an interaction of expectedness and valence affecting the EEG signal in the latency range of the FRN. This result supports the RL theory that the FRN is affected by a signed RPE signal. The FRN modulation by expectedness was stronger after positive feedback than after negative feedback. Hence, one could also interpret the present findings in the context of a RewP. Since this valence-specific effect occurs only in interaction with expectedness, this interpretation does not seem straight forward to us. In other words, EEG dynamics in the time range of the FRN are more modulated by outcome expectancy after positive compared to negative feedback. RPEs are therefore stronger represented and have a larger "dynamic range" during positive events than during negative events. In this case, the RPE appears to be driven by surprise. In contrast, when the RPE is driven by valence, we found a stronger, later, and more parietal modulation of the FRN by valence for unexpected events than for expected events. This finding rather supports recent evidence suggesting that the FRN reflects some combination of reward- and salience-prediction error encoding (Glazer and Nusslock, 2021). In line with that, new studies state that the signal in the latency range of the FRN reflects independent processing of both better-than-expected and worse-than-expected outcomes (Bernat et al., 2015, 2008; Foti et al., 2015; Hoy et al., 2021). The FRN is proposed to reflect the neural response to a negative RPE (losses) associated with theta band oscillatory perturbations (Cavanagh et al., 2012, 2010; Cavanagh and Frank, 2014; Cavanagh and Shackman, 2015), whereas the RewP is proposed to reflect the neural response to a positive RPE (wins) associated with delta band activities (Cavanagh, 2015). Unfortunately, in the present study, there are some limitations that restrict the interpretation of the RPE, particularly the differentiation into positive and negative RPEs. Due to the task design, the probability and valence of the feedback are intertwined.

4.2. Factors influencing the later feedback-related neuronal signal

Results for the neuronal signal at later latencies show also an influence of expectedness and valence. Regarding surprise, there is a sustained centroparietal effect from around 300 ms on (see Fig. 5). From 340 ms after feedback, a valence-specific frontoparietal positive covariation appears and finds its peak at 380 ms.

Concerning the P3 complex, the influence of global surprise could be replicated (de Bruijn et al., 2004; Fischer and Ullsperger, 2013; Mars et al., 2008): we showed a dependence of the neuronal signal during the time window of the P3b at centroparietal areas on expectedness. Valence elicited a frontoparietal effect from 340 ms on. This P3a-pattern could therefore represent a stimulus-driven attention mechanism. Furthermore, the P3 complex was most positive for unexpected positive-feedback outcomes. This finding is consistent with the results of Hajcak et al. (2007) and Severo et al. (2018). Walentowska et al. (2019) had similar findings: the P3b amplitude was larger for positive than negative feedback in unexpected events. Because surprising positive events can be very helpful in increasing the performance, this phenomenon could be interpreted as a goal-relevant action-value-updating of this specific feedback. Additionally, we addressed surprise on a more trial-by-trial basis and examined the impact of a locally surprising event. In line with previous evidence (Mars et al., 2008; Nieuwenhuis et al., 2005; Squires et al., 1976), results show a dependence of the P3 complex to local surprise in a way, that the P3 is more positive when local deviants appear.

4.3. Link between FRN and behavioral adaptation

Concerning behavioral adaptation, an association between the size of the FRN and the amount of behavioral adjustment in the following trial in combination with feedback valence was assumed: after negative feedback, a stronger effect on the neuronal signal in the time window of the FRN is expected to be associated with a bigger change in reaction time than after positive feedback. In a more exploratory way, we created a measure for behavioral adaptation that also depicts performance improvement and decline. Results show only a small association between adaptation after feedback and the neuronal signal during the time window of the FRN both overall trials and for trials with negative feedback, mostly at parietal electrodes. Previous research was able to link the FRN to behavioral adaptations depending on feedback valence and expectedness (Arbel et al., 2013; Cavanagh, 2015; Holroyd and Krigolson, 2007). One reason why we could not reproduce these findings is the nature of the feedback used in the present task. The feedback contained information about the correctness of the response but did not tell the participants in which direction to adjust their behavior in order to improve their performance in the upcoming trial. At the same

time, our measure of behavioral adaptation did contain directional information about whether one is getting closer or further away from the correct response, and thus did not correspond to the information content of the feedback itself. In order to use feedback profitably, the information content is crucial. It has already been shown that this also affects the neuronal signal (Cockburn and Holroyd, 2018). Future experiments should therefore work with differentially informative feedback and corresponding outcome measures to more specifically capture the relationship between the feedback-processing neuronal signals and behavioral consequences. The unspecific association between behavioral adaptations and feedback-related EEG activity in our task might reflect participants' attempt to adjust their behavior in an exploratory manner following negative feedback. The dependence of behavioral adaptation on both feedback valence and expectedness might suggest that participants infer that it is adaptive to adjust their behavior more after unexpected negative feedback. In this task-state, the target time window is wider, hence larger adjustments are more likely to improve behavior. Because participants are not told whether their time estimation was too fast or too slow, they are forced to randomly adjust their behavior after negative feedback and try to memorize their time estimation after positive feedback. This process could be reflected in the sustained parietal positive response seen after positive feedback. For the present study, however, this assumption has to remain a tentative explanation.

In line with the findings mentioned above (4.1), adaptive behavior and learning after feedback can have different functions depending on the type of RPE: an unsigned PE may enhance selective attention based on known task rules (Danielmeier et al., 2015, 2011; King et al., 2010), while a signed PE determines the direction of reinforcement learning, that is, to repeat or avoid an action (Ullsperger et al., 2014b). Arbel et al. (2013) showed that the FRN elicited by negative feedback was not correlated with long-term learning outcomes, whereas positive-feedback-associated FRN was correlated with the learning outcomes. In contrast, Cavanagh (2015) hypothesized a differentiation in hierarchically distinct types of prediction error, where delta band activity linked to a rewarding event motivates immediate behaviors, while theta band activity linked to punishing events initiates long-term behavioral adjustments (Cavanagh and Shackman, 2015). In the present study, we demonstrate a small effect of the interaction of consecutive behavioral adaptation with outcome expectedness on the neuronal signal between 240 and 280 ms for trials with negative feedback. This may provide evidence for the connection between negative RPE and behavioral adjustments. Nevertheless, the FRN varies due to different feedback characteristics and the amount of feedback information (Cockburn and Holroyd, 2018) and is therefore highly task dependent. This could be one reason for inconsistencies in existing evidence. Studies finding inter-individual differences (van Noordt and Segalowitz, 2012) or studies related to mental disorders (Endrass et al., 2013; Keren et al., 2018; Webb et al., 2017) also show that the FRN does not reflect a monolithic block with only one unique functional interpretation. Rather, the task, context, etc., must be considered to characterize the factors that contribute to the FRN. These contributions and their representations may vary independently (Stewardson and Sambrook, 2021), leading to variations in ERPs. This can even lead to latency shifts in the individual effects, making it difficult to unambiguously assign FRN and P3. Therefore, the task should always be considered when interpreting different findings concerning the FRN and adaptive behavior.

4.4. Link between P3 and behavioral adaptation

Since the feedback-related P3 had been associated with behavioral adaptation (Fischer and Ullsperger, 2013; Jepma et al., 2018, 2016), the P3 amplitude could be expected to correlate positively with changes in behavioral performance after feedback. Surprisingly, there was a contrarian association between behavioral adaptation and the neuronal signal in the P3 time frame at frontoparietal areas (see Fig. 5): the neuronal signal appears less positive when behavioral adaptation to the next trial is greater, i.e. that performance has improved. Nassar et al. (2019) and Kirschner et al. (2021) predicted adjustments in behavior based on the amplitude of the P3, but as a function of the source of surprise. If the surprise was uninformative, the P3 negatively predicted learning. As mentioned earlier, the feedback in the present study was uninformative in a way that it was not directional. Thus, it can be concluded that the counterintuitive association between P3 and behavioral adjustment in the present study may reflect the negative prediction from above (Kirschner et al., 2021; Nassar et al., 2019). Additionally, Cavanagh (2015) found an association between the P3 complex and behavioral adaptation: delta band phase dynamics observed in the P3 appear to be involved in strategic behavioral adjustments like the degree of response time speeding. Interpretation of the authors suggests that the processes underlying FRN and P3 reflect hierarchically different levels of prediction errors, reward and state prediction errors, respectively. Whereas reward prediction errors give information to a model-free learner on a trial-and-error basis, state prediction errors inform model-based systems by more complex forward predictions. If the P3 is modulated by state prediction errors and therefore depends on an agents' decision-making policy, a richer learning environment may be needed to reveal the relationship between behavioral adaptation and the neuronal signal during the corresponding time frame (like Chase et al., 2011).

Taken together, the investigated ERP deflections are not only due to single influencing factors, but are complex representations composed of several influencing components. As Fig. 5 clearly shows, even within FRN latency ranges there are temporally and spatially distinguishable effects that are difficult to characterize using an ERP averaging approach. Also, previous methodological considerations (Glazer et al., 2018; Williams et al., 2020) indicate the difficulty to isolate the FRN and confounds arising from component overlap. Therefore, they underline the importance of teasing apart the stages of feedback processing to integrate individual reward-related ERPs in a more holistic view and to capture the broader temporal dynamics (Foti and Weinberg, 2018; Glazer et al., 2018). There are already some attempts to do so (Gheza et al., 2018; Sambrook and Goslin, 2016). Moreover, time-frequency analysis could help future research identify and differentiate cognitive processes underlying different types of RPE and their roles in behavioral adjustments to improve performance.

4.5. Limitations

Methodological limitations include that feedback-related EEG dynamics may have been modulated by offset-related visual ERPs after 350 ms past feedback, but it is unlikely to affect our results with respect to the regressors of interest. Additionally, previous findings have shown an influence of valence effects on the amplitude of the FRN depending on the perceptual salience of the feedback stimuli (Liu et al., 2014). In the present study, we cannot rule out this effect because feedback color was not counterbalanced across participants.

5. Conclusion

In the present study, we disentangled the functional relevance of independent contributions to electrophysiological correlates of feedback processing in a big sample of $N = 992$ participants by using a novel approach in EEG analysis and a time estimation paradigm. While we have previously used instrumental learning tasks (Burnside et al., 2019; Fischer and Ullsperger, 2013; Kirschner et al., 2021), we were able to replicate typical feedback-related components with the present task despite it involves less opportunities to adapt behavior. The results of the present study support the view that the FRN is driven by a signed RPE and furthermore influenced by global surprise. Depending on what drives the RPE most –expected value or obtained outcome–, different modulations of the FRN are possible. Whereas the FRN was less influenced by global and local surprise, unexpected events elicited a larger

P3b. An association between behavioral adjustments and the P3 might indicate a representation of different RPE levels and types within the components involved in feedback processing. With the help of a big sample size and a regression approach that allows the simultaneous investigation of multiple independent variables, we obtain information on the temporal and spatial variance of the contributing effects on the neuronal signal.

Funding information

This research was supported by the Deutsche Forschungsgemeinschaft (DFG; KL 2337/2-1, KL2337/2-3, and UL 196/3-3.) and AGF was supported by a grant from the CBBS ScienceCampus financed by the Leibniz Association (SAS-2015-LIN-LWC).

Data and code availability

The conditions of our informed consent form do not permit public archiving of the raw data because participants did not provide sufficient consent. Researchers who wish to access processed and anonymized data from a reasonable perspective should contact the corresponding author. Data will be released to researchers if it is possible under the terms of the GDPR (General Data Protection Regulation).

The code of the toolbox we used for the regression analysis can be found here: http://www.adrianfischer.de/teaching.html.

Declaration of Competing Interest

The authors declare that they have no known competing financial interests or personal relationships that could have appeared to influence the work reported in this paper.

Credit authorship contribution statement

Franziska Kirsch: Conceptualization, Methodology, Data curation, Formal analysis, Visualization, Writing – original draft. **Hans Kirschner:** Conceptualization, Methodology, Data curation, Formal analysis, Visualization, Writing – review & editing. **Adrian G. Fischer:** Software, Formal analysis, Methodology, Writing – review & editing. **Tilmann A. Klein:** Conceptualization, Methodology, Funding acquisition, Resources, Supervision, Writing – review & editing. **Markus Ullsperger:** Conceptualization, Methodology, Funding acquisition, Resources, Supervision, Writing – review & editing.

Acknowledgments

The authors thank Maria Dreyer for her help with data acquisition, and B. Franke and G. Fernandez for their support in recruiting the Nijmegen sample.

References

Alexander, W.H., Brown, J.W., 2011. Medial prefrontal cortex as an action-outcome predictor. Nat. Neurosci. 14, 1338–1344. doi:10.1038/nn.2921.

Arbel, Y., Goforth, K., Donchin, E., 2013. The good, the bad, or the useful? The examination of the relationship between the feedback-related negativity (FRN) and long-term learning outcomes. J. Cogn. Neurosci. 25, 1249–1260. doi:10.1162/jocn_a_00385.

Baker, T.E., Holroyd, C.B., 2011. Dissociated roles of the anterior cingulate cortex in reward and conflict processing as revealed by the feedback error-related negativity and N200. Biol. Psychol. 87, 25–34. doi:10.1016/j.biopsycho.2011.01.010.

Bernat, E.M., Nelson, L.D., Baskin-Sommers, A.R., 2015. Time-frequency theta and delta measures index separable components of feedback processing in a gambling task. Psychophysiology 52, 626–637. doi:10.1111/psyp.12390.

Bernat, E.M., Nelson, L.D., Holroyd, C.B., Gehring, W.J., Patrick, C.J., 2008. Separating cognitive processes with principal components analysis of EEG time-frequency distributions. In: *Advanced Signal Processing Algorithms, Architectures, and Implementations XVIII*. Optical Engineering + Applications, San Diego, California, USA. SPIE, p. 70740S Sunday 10 August 2008.

de Bruijn, E.R.A., Mars, R.B., Hulstijn, W., 2004. 'It wasn't me… or was it?' How false feedback effects performance. In: Ullsperger, M., Falkenstein, M. (Eds.), Errors, Conflicts, and the Brain. Current opinions on Performance Monitoring. Max Planck Institute of Cognitive Neuroscience, Leipzig, Germany, pp. 118–124.

Burnside, R., Fischer, A.G., Ullsperger, M., 2019. The feedback-related negativity indexes prediction error in active but not observational learning. Psychophysiology 56, e13389. doi:10.1111/psyp.13389.

Cavanagh, J.F., 2015. Cortical delta activity reflects reward prediction error and related behavioral adjustments, but at different times. Neuroimage 110, 205–216. doi:10.1016/j.neuroimage.2015.02.007.

Cavanagh, J.F., Bismark, A.W., Frank, M.J., Allen, J.J.B., 2019. Multiple dissociations between comorbid depression and anxiety on reward and punishment processing: evidence from computationally informed EEG. Comput Psychiatr 3, 1–17. doi:10.1162/cpsy_a_00024.

Cavanagh, J.F., Figueroa, C.M., Cohen, M.X., Frank, M.J., 2012. Frontal theta reflects uncertainty and unexpectedness during exploration and exploitation. Cereb. Cortex 22, 2575–2586. doi:10.1093/cercor/bhr332.

Cavanagh, J.F., Frank, M.J., 2014. Frontal theta as a mechanism for cognitive control. Trends Cogn. Sci. 18, 414–421. doi:10.1016/j.tics.2014.04.012.

Cavanagh, J.F., Frank, M.J., Klein, T.J., Allen, J.J.B., 2010. Frontal theta links prediction errors to behavioral adaptation in reinforcement learning. Neuroimage 49, 3198–3209. doi:10.1016/j.neuroimage.2009.11.080.

Cavanagh, J.F., Shackman, A.J., 2015. Frontal midline theta reflects anxiety and cognitive control: meta-analytic evidence. J. Physiol. Paris 109, 3–15. doi:10.1016/j.jphysparis.2014.04.003.

Chase, H.W., Swainson, R., Durham, L., Benham, L., Cools, R., 2011. Feedback-related negativity codes prediction error but not behavioral adjustment during probabilistic reversal learning. J. Cogn. Neurosci. 23, 936–946. doi:10.1162/jocn.2010.21456.

Cockburn, J., Holroyd, C.B., 2018. Feedback information and the reward positivity. Int. J. Physiol. 132, 243–251. doi:10.1016/j.ijpsycho.2017.11.017.

Cohen, M.X., Ranganath, C., 2007. Reinforcement learning signals predict future decisions. J. Neurosci. 27, 371–378. doi:10.1523/JNEUROSCI.4421-06.2007.

Danielmeier, C., Allen, E.A., Jocham, G., Onur, O.A., Eichele, T., Ullsperger, M., 2015. Acetylcholine mediates behavioral and neural post-error control. Curr. Biol. 25, 1461–1468. doi:10.1016/j.cub.2015.04.022.

Danielmeier, C., Eichele, T., Forstmann, B.U., Tittgemeyer, M., Ullsperger, M., 2011. Posterior medial frontal cortex activity predicts post-error adaptations in task-related visual and motor areas. J. Neurosci. 31, 1780–1789. doi:10.1523/JNEUROSCI.4299-10.2011.

Delorme, A., Makeig, S., 2004. EEGLAB: an open source toolbox for analysis of single-trial EEG dynamics including independent component analysis. J. Neurosci. Methods 134, 9–21. doi:10.1016/j.jneumeth.2003.10.009.

Delorme, A., Sejnowski, T., Makeig, S., 2007. Enhanced detection of artifacts in EEG data using higher-order statistics and independent component analysis. Neuroimage 34, 1443–1449. doi:10.1016/j.neuroimage.2006.11.004.

Donchin, E., Coles, M.G.H., 1998. Context updating and the P300. Behav. Brain Sci. 21, 152–154. doi:10.1017/S0140525x98230950.

Donkers, F.C., van Boxtel, G.J., 2005. Mediofrontal negativities to averted gains and losses in the slot-machine task. J. Psychophysiol. 19, 256–262. doi:10.1027/0269-8803.19.4.256.

Endrass, T., Koehne, S., Riesel, A., Kathmann, N., 2013. Neural correlates of feedback processing in obsessive-compulsive disorder. J. Abnorm. Psychol. 122, 387–396. doi:10.1037/a0031496.

Ferdinand, N.K., Mecklinger, A., Kray, J., Gehring, W.J., 2012. The processing of unexpected positive response outcomes in the mediofrontal cortex. J. Neurosci. 32, 12087–12092. doi:10.1523/JNEUROSCI.1410-12.2012.

Fischer, A.G., Danielmeier, C., Villringer, A., Klein, T.A., Ullsperger, M., 2016. Gender influences on brain responses to errors and post-error adjustments. Sci. Rep. 6, 24435. doi:10.1038/srep24435.

Fischer, A.G., Ullsperger, M., 2013. Real and fictive outcomes are processed differently but converge on a common adaptive mechanism. NeuronNeuron 79, 1243–1255. doi:10.1016/j.neuron.2013.07.006.

Foti, D., Weinberg, A., 2018. Reward and feedback processing: state of the field, best practices, and future directions. Int. J. Physiol. 132, 171–174. doi:10.1016/j.ijpsycho.2018.08.006.

Foti, D., Weinberg, A., Bernat, E.M., Proudfit, G.H., 2015. Anterior cingulate activity to monetary loss and basal ganglia activity to monetary gain uniquely contribute to the feedback negativity. Clin. Neurophysiol. 126, 1338–1347. doi:10.1016/j.clinph.2014.08.025.

Gentsch, A., Ullsperger, P., Ullsperger, M., 2009. Dissociable medial frontal negativities from a common monitoring system for self- and externally caused failure of goal achievement. NeuroimageNeuroimage 47, 2023–2030. doi:10.1016/j.neuroimage.2009.05.064.

Gheza, D., Paul, K., Pourtois, G., 2018. Dissociable effects of reward and expectancy during evaluative feedback processing revealed by topographic ERP mapping analysis. Int. J. Physiol. 132, 213–225. doi:10.1016/j.ijpsycho.2017.11.013.

Glazer, J., Kelley, N.J., Pornpattananangkul, N., Mittal, V.A., Nusslock, R., 2018. Beyond the FRN: broadening the time-course of EEG and ERP components implicated in reward processing. Int. J. Physiol. 132, 184–202. doi:10.1016/j.ijpsycho.2018.02.002.

Glazer, J., Nusslock, R., 2021. Outcome valence and stimulus frequency affect neural responses to rewards and punishments. Psychophysiology e13981. doi:10.1111/psyp.13981.

Gruendler, T.O.J., Ullsperger, M., Huster, R.J., 2011. Event-related potential correlates of performance-monitoring in a lateralized time-estimation task. PLoS ONE 6, e25591. doi:10.1371/journal.pone.0025591.

Hajcak, G., Moser, J.S., Holroyd, C.B., Simons, R.F., 2007. It's worse than you thought: the feedback negativity and violations of reward prediction in gambling tasks. Psychophysiology 905–912. doi:10.1111/j.1469-8986.2007.00567.x.

Hauser, T.U., Iannaccone, R., Stämpfli, P., Drechsler, R., Brandeis, D., Walitza, S., Brem, S., 2014. The feedback-related negativity (FRN) revisited: new insights into the localization, meaning and network organization. Neuroimage 84, 159–168. doi:10.1016/j.neuroimage.2013.08.028.

Holroyd, C.B., Coles, M.G.H., 2002. The neural basis of human error processing: reinforcement learning, dopamine, and the error-related negativity. Psychol. Rev. 109, 679–709. doi:10.1037//0033-295X.109.4.679.

Holroyd, C.B., Krigolson, O.E., 2007. Reward prediction error signals associated with a modified time estimation task. Psychophysiology 44, 913–917. doi:10.1111/j.1469-8986.2007.00561.x.

Holroyd, C.B., Pakzad-Vaezi, K.L., Krigolson, O.E., 2008. The feedback correct-related positivity: sensitivity of the event-related brain potential to unexpected positive feedback. Psychophysiology 45, 688–697. doi:10.1111/j.1469-8986.2008.00668.x.

Hoy, C.W., Steiner, S.C., Knight, R.T., 2021. Single-trial modeling separates multiple overlapping prediction errors during reward processing in human EEG. Commun. Biol. 4, 910. doi:10.1038/s42003-021-02426-1.

Intriligator, J., Polich, J., 1994. On the relationship between background EEG and the P300 event-related potential. Biol. Psychol. 37, 207–218. doi:10.1016/0301-0511(94)90003-5.

Jepma, M., Brown, S.B.R.E., Murphy, P.R., Koelewijn, S.C., de Vries, B., van den Maagdenberg, A.M., Nieuwenhuis, S., 2018. Noradrenergic and cholinergic modulation of belief updating. J. Cogn. Neurosci. 30, 1803–1820. doi:10.1162/jocn_a_01317.

Jepma, M., Murphy, P.R., Nassar, M.R., Rangel-Gomez, M., Meeter, M., Nieuwenhuis, S., 2016. Catecholaminergic regulation of learning rate in a dynamic environment. PLoS Comput. Biol. 12, e1005171. doi:10.1371/journal.pcbi.1005171.

Jocham, G., Neumann, J., Klein, T.A., Danielmeier, C., Ullsperger, M., 2009. Adaptive coding of action values in the human rostral cingulate zone. J. Neurosci. 29, 7489–7496. doi:10.1523/JNEUROSCI.0349-09.2009.

Johnson, R., 1986. A triarchic model of P300 amplitude. Psychophysiology 23, 367–384. doi:10.1111/j.1469-8986.1986.tb00649.x.

Kamarajan, C., Porjesz, B., Rangaswamy, M., Tang, Y., Chorlian, D.B., Padmanabhapillai, A., Saunders, R., Pandey, A.K., Roopesh, B.N., Manz, N., Stimus, A.T., Begleiter, H., 2009. Brain signatures of monetary loss and gain: outcome-related potentials in a single outcome gambling task. Behav. Brain Res. 197, 62–76. doi:10.1016/j.bbr.2008.08.011.

Keren, H., O'Callaghan, G., Vidal-Ribas, P., Buzzell, G.A., Brotman, M.A., Leibenluft, E., Pan, P.M., Meffert, L., Kaiser, A., Wolke, S., Pine, D.S., Stringaris, A., 2018. Reward processing in depression: a conceptual and meta-analytic review across fMRI and EEG studies. Am. J. Psychiatry 175, 1111–1120. doi:10.1176/appi.ajp.2018.17101124.

King, J.A., Korb, F.M., von Cramon, D.Y., Ullsperger, M., 2010. Post-error behavioral adjustments are facilitated by activation and suppression of task-relevant and task-irrelevant information processing. J. Neurosci. 30, 12759–12769. doi:10.1523/JNEUROSCI.3274-10.2010.

Kirschner, H., Fischer, A.G., Ullsperger, M., 2021. Feedback-related EEG dynamics separately reflect decision parameters, biases, and future choices. preprint. doi:10.1101/2021.05.10.443374.

Krigolson, O.E., 2018. Event-related brain potentials and the study of reward processing: methodological considerations. Int. J. Physiol. 132, 175–183. doi:10.1016/j.ijpsycho.2017.11.007.

Liu, Y., Nelson, L.D., Bernat, E.M., Gehring, W.J., 2014. Perceptual properties of feedback stimuli influence the feedback-related negativity in the flanker gambling task. Psychophysiology 51, 782–788. doi:10.1111/psyp.12216.

Mars, R.B., Debener, S., Gladwin, T.E., Harrison, L.M., Haggard, P., Rothwell, J.C., Bestmann, S., 2008. Trial-by-trial fluctuations in the event-related electroencephalogram reflect dynamic changes in the degree of surprise. J. Neurosci. 28, 12539–12545. doi:10.1523/JNEUROSCI.2925-08.2008.

Miltner, W.H., Braun, C.H., Coles, M.G.H., 1997. Event-related brain potentials following incorrect feedback in a time-estimation task: evidence for a "generic" neural system for error detection. J. Cogn. Neurosci. 9, 788–798. doi:10.1162/jocn.1997.9.6.788.

Nassar, M.R., Bruckner, R., Frank, M.J., 2019. Statistical context dictates the relationship between feedback-related EEG signals and learning. Elife 8. doi:10.7554/eLife.46975.

Nieuwenhuis, S., Aston-Jones, G., Cohen, J.D., 2005. Decision making, the P3, and the locus coeruleus-norepinephrine system. Psychol. Bull. 131, 510–532. doi:10.1037/0033-2909.131.4.510.

Nieuwenhuis, S., Holroyd, C.B., Mol, N., Coles, M.G.H., 2004. Reinforcement-related brain potentials from medial frontal cortex: origins and functional significance. Neurosci. Biobehav. Rev. 28, 441–448. doi:10.1016/j.neubiorev.2004.05.003.

Palmer, J.A., Kreutz-Delgado, K., Makeig, S., 2012. AMICA: An adaptive Mixture of Independent Component Analyzers with Shared Components. Swartz Center for Computational Neuroscience, University of California San Diego Tech. Rep..

Polich, J., 2007. Updating P300: an integrative theory of P3a and P3b. Clin. Neurophysiol. 118, 2128–2148. doi:10.1016/j.clinph.2007.04.019.

Proudfit, G.H., 2015. The reward positivity: from basic research on reward to a biomarker for depression. Psychophysiology 52, 449–459. doi:10.1111/psyp.12370.

Sambrook, T.D., Goslin, J., 2015. A neural reward prediction error revealed by a meta-analysis of ERPs using great grand averages. Psychol. Bull. 141, 213–235. doi:10.1037/bul0000006.

Sambrook, T.D., Goslin, J., 2016. Principal components analysis of reward prediction errors in a reinforcement learning task. Neuroimage 124, 276–286. doi:10.1016/j.neuroimage.2015.07.032.

San Martín, R., 2012. Event-related potential studies of outcome processing and feedback-guided learning. Front. Hum. Neurosci. 6, 304. doi:10.3389/fnhum.2012.00304.

Sato, A., Yasuda, A., Ohira, H., Miyawaki, K., Nishikawa, M., Kumano, H., Kuboki, T., 2005. Effects of value and reward magnitude on feedback negativity and P300. Neuroreport 16, 407–411. doi:10.1097/00001756-200503150-00020.

Severo, M.C., Walentowska, W., Moors, A., Pourtois, G., 2018. Goals matter: amplification of the motivational significance of the feedback when goal impact is increased. Brain Cogn. 56–72. doi:10.1016/j.bandc.2018.11.002.

Squires, K.C., Wickens, C., Squires, N.K., Donchin, E., 1976. The effect of stimulus sequence on the waveform of the cortical event-related potential. Science 193, 1142–1146. doi:10.1126/science.959831.

Stewardson, H.J., Sambrook, T.D., 2021. Reward, salience, and agency in event-related potentials for appetitive and aversive contexts. Cereb. Cortex 31, 5006–5014. doi:10.1093/cercor/bhab137/6279867.

Talmi, D., Atkinson, R., El-Deredy, W., 2013. The feedback-related negativity signals salience prediction errors, not reward prediction errors. J. Neurosci. 33, 8264–8269. doi:10.1523/JNEUROSCI.5695-12.2013.

Toyomaki, A., Murohashi, H., 2005. Discrepancy between feedback negativity and subjective evaluation in gambling. Neuroreport 16, 1865–1868. doi:10.1097/01.wnr.0000185962.96217.36.

Ullsperger, M., 2017. Neural bases of performance monitoring. In: Egner, T. (Ed.), The Wiley Handbook of Cognitive Control. John Wiley & Sons, Ltd, Chichester, UK, pp. 292–313 vol. 14.

Ullsperger, M., Danielmeier, C., Jocham, G., 2014a. Neurophysiology of performance monitoring and adaptive behavior. Physiol. Rev. 94, 35–79. doi:10.1152/physrev.00041.2012.

Ullsperger, M., Fischer, A.G., Nigbur, R., Endrass, T., 2014b. Neural mechanisms and temporal dynamics of performance monitoring. Trends Cogn. Sci. 18, 259–267. doi:10.1016/j.tics.2014.02.009.

van Boxtel, G.J., 2004. The use of the subtraction technique in the psychophysiology of response inhibition and conflict. In: Ullsperger, M., Falkenstein, M. (Eds.), Errors, Conflicts, and the Brain. Current opinions on Performance Monitoring. Max Planck Institute of Cognitive Neuroscience, Leipzig, Germany, pp. 219–225.

van Noordt, S.J.R., Segalowitz, S.J., 2012. Performance monitoring and the medial prefrontal cortex: a review of individual differences and context effects as a window on self-regulation. Front Hum Neurosci 6, 197. doi:10.3389/fnhum.2012.00197.

Verleger, R., 1997. On the utility of P3 latency as an index of mental chronometry. Psychophysiology 34, 131–156. doi:10.1111/j.1469-8986.1997.tb02125.x.

Verleger, R., Jaskowski, P., Wauschkuhn, B., 1994. Suspense and surprise: on the relationship between expectancies and P3. Psychophysiology 31, 359–369. doi:10.1111/j.1469-8986.1994.tb02444.x.

Viola, F.C., Thorne, J., Edmonds, B., Schneider, T., Eichele, T., Debener, S., 2009. Semi-automatic identification of independent components representing EEG artifact. Clin. Neurophysiol. 120, 868–877. doi:10.1016/j.clinph.2009.01.015.

Walentowska, W., Moors, A., Paul, K., Pourtois, G., 2016. Goal relevance influences performance monitoring at the level of the FRN and P3 components. Psychophysiology 1020–1033. doi:10.1111/psyp.12651.

Walentowska, W., Severo, M.C., Moors, A., Pourtois, G., 2019. When the outcome is different than expected: subjective expectancy shapes reward prediction error at the FRN level. Psychophysiology 56, e13456. doi:10.1111/psyp.13456.

Walsh, M.M., Anderson, J.R., 2012. Learning from experience: event-related potential correlates of reward processing, neural adaptation, and behavioral choice. Neurosci. Biobehav. Rev. 36, 1870–1884. doi:10.1016/j.neubiorev.2012.05.008.

Webb, C.A., Auerbach, R.P., Bondy, E., Stanton, C.H., Foti, D., Pizzagalli, D.A., 2017. Abnormal neural responses to feedback in depressed adolescents. J. Abnorm. Psychol. 126, 19–31. doi:10.1037/abn0000228.

Williams, C.C., Ferguson, T.D., Hassall, C.D., Abimbola, W., Krigolson, O.E., 2020. The ERP, frequency, and time-frequency correlates of feedback processing: insights from a large sample study. Psychophysiology e13722. doi:10.1111/psyp.13722.

Yeung, N., Holroyd, C.B., Cohen, J.D., 2005. ERP correlates of feedback and reward processing in the presence and absence of response choice. Cereb. Cortex 15, 535–544. doi:10.1093/cercor/bhh153.

Yeung, N., Sanfey, A.G., 2004. Independent coding of reward magnitude and valence in the human brain. J. Neurosci. 24, 6258–6264. doi:10.1523/JNEUROSCI.4537-03.2004.